ACCELERATION INSENSITIVE HEMISPHERICAL SHELL RESONATORS USING POP-UP RINGS

Mustafa Mert Torunbalci, Sen Dai, Ajay Bhat and Sunil A. Bhave
OxideMEMS Lab, Purdue University, West Lafayette, IN, USA

ABSTRACT

This work introduces DICE (Deep Isotropic Chemical Etching) process for fabrication of highly symmetric 3D Hemispherical Shell Resonators (HSR) based on HNA etching of <111> silicon using a pop-up ring mask. The proposed method is used to fabricate 650 nm thick SiO_2 hemispherical shell with a diameter of 180 µm, demonstrating a 3D symmetry of 99%. The quality factor (Q) of the wine glass n=2 mode is measured as 31542 at 100 kHz with a frequency mismatch of 512 Hz ($\Delta f/f_r$=0.5%) between the two n=2 degenerate modes. COMSOL simulations show that a symmetric shell resonator has simultaneous shock insensitivity to in-plane and out-of-plane acceleration.

INTRODUCTION

Hemispherical Resonator Gyroscopes (HRG) are made of a hemispherical shell anchored by a thick stem and have been used for navigation and space applications due to their excellent sensitivity as well as reliable operation over time. Northrop Grumman manufactures the world's most sensitive macro HRG, but it's only used in satellites because of their extreme sensitivity to the external vibrations. Recently, they have started manufacturing mm-scale HRG to increase the operation frequency for using them in high-speed projectiles [1]. However, these quartz gyroscopes are extremely costly due to the serial manufacturing, polishing, and assembly process. Micro-HSRs and gyroscopes have been recently demonstrated by using different microfabrication processes: a) deposition of structural thin-films on pre-defined molds [2-5] or b) blow molding the resonator [6, 7]. It is experimentally evident that the 3D resonator shape (anchor positioned far away from the plane of maximum vibration) is sufficient to achieve high Q and extremely small mode-frequency split. Therefore, the micro-scale HSRs evolved into "bird-baths" [7], cylinders [8], bubbles [9] and "pierced shell" [10] resonators. However, there is one key advantage of the perfect HSR that none of these designs retain-simultaneous insensitivity to x and z axis accelerations during whole angle operation.

In this paper, we present a novel way of fabricating highly symmetric and smooth silicon molds based on HNA etching of <111> silicon using a pop-up ring mask. Proper design of these pop-up rings allows excellent control of lateral and vertical etch rates, enabling the fabrication of super-symmetric HSRs in the desired dimensions. COMSOL analysis has been done to analyze the acceleration sensitivity of the different HSR structures. These analysis exhibit that HSRs fabricated with the pop-up ring mask are more immune to external acceleration/shock, demonstrating an excellent vibration insensitivity.

DICE

Figure 1 (a-d) compares masking approaches for silicon mold fabrication. Small isotropic molds in <111> silicon was already demonstrated in [11] but the key breakthrough for achieving larger shells is to draw concentric rings in the silicon nitride mask layer instead of a pin-hole. These rings pop-up and widen the etch aperture as etch-depth increases, thereby yielding a large radius super-symmetric mold. Optimum number of pop-up rings should be designed to reach desired dimensions since large number of pop-up rings fly-off too fast, still causing shallow molds. Small/large pin-holes either become diffusion limited or have a poor aspect ratio.

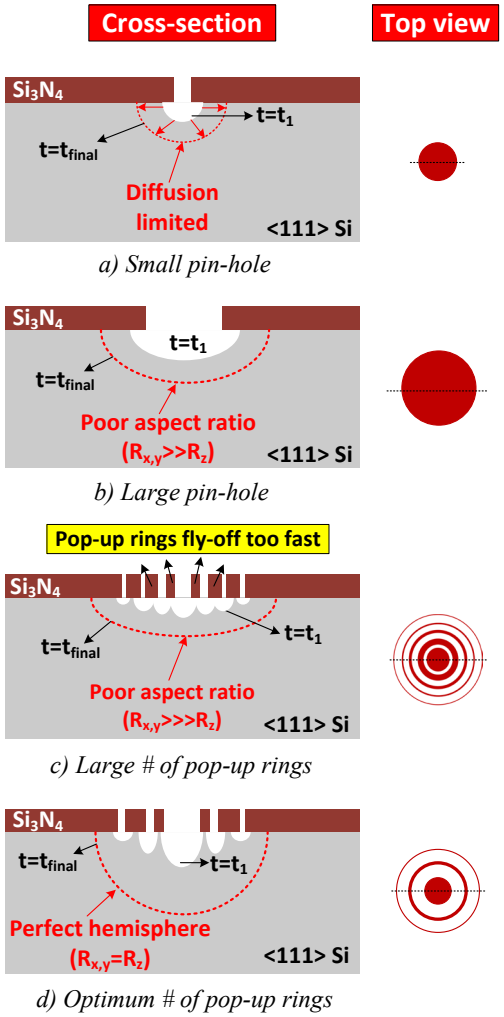

Figure 1: Masking approaches for silicon mold fabrication: a) Small pin-hole (~5µm) becomes diffusion limited at a short depth, b) Large pin-hole (~50µm) creates shallow mold because initial etch depression is wide, (c) Multiple pop-up rings fly-off too fast, (d) Perfect hemisphere with optimum number of pop-up rings and optimum spacing.

Figure 2 (a-d) presents main process steps for the HSRs with the pop-up ring mask. Pop-up ring mask is formed on a <111> silicon substrate by etching a 300 nm thick LPCVD silicon nitride using RIE. Next, a hemisphere mold is formed by HNA etching of silicon using the pop-up ring mask. HNA concentration is optimized to be 1:4:1 in order to obtain the smoothest surface. Three concentric pop-up rings with a decreasing spacing allow excellent control of lateral and vertical etch rates to reach the target depth of 100 µm. However, pop-up mask design can be easily modified by increasing the number of rings by preserving the optimum spacing in order to fabricate mm-scale HSR devices while maintaining the symmetry of the mold. Next, a 650 nm thick SiO_2 structural layer is thermally grown and then patterned with RIE. Just a thin layer of photoresist is used to fill the molds to get rid of the lips in [11], eliminating the undesired mechanical modes during the operation. Finally, HSRs are released by XeF_2. The anchor dimensions of the HSRs are controlled by a timed-release process. Figure 3 shows SEMs of HSR fabricated using the pop-up mask, verifying the super-symmetry of the fabricated HSRs.

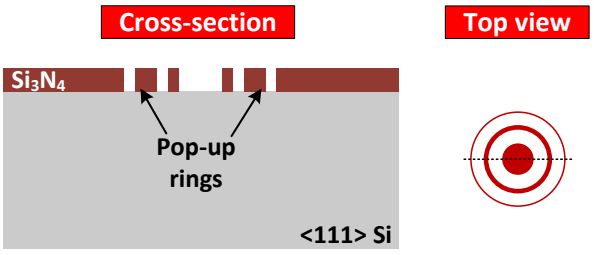

a) Pop-up rings on Si_3N_4 with RIE

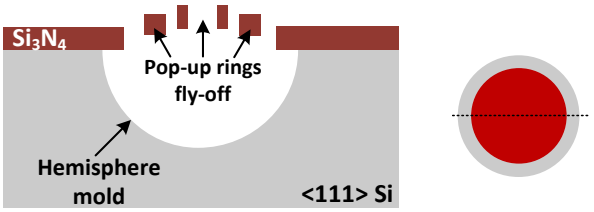

b) HNA etching of silicon, pop-up rings fly-off

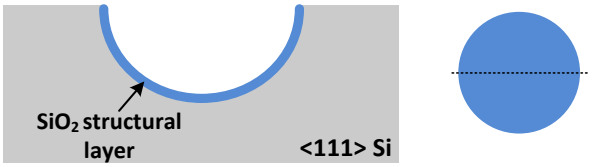

c) Thermal oxidation and patterning with RIE

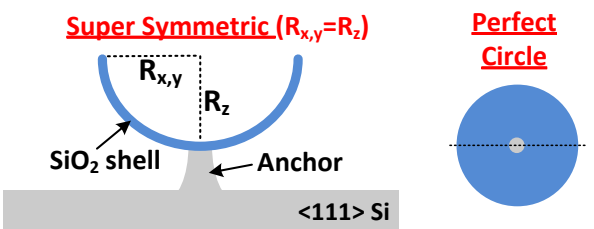

d) XeF_2 release

Figure 2: Key process steps of HSRs fabricated with the pop-up ring mask.

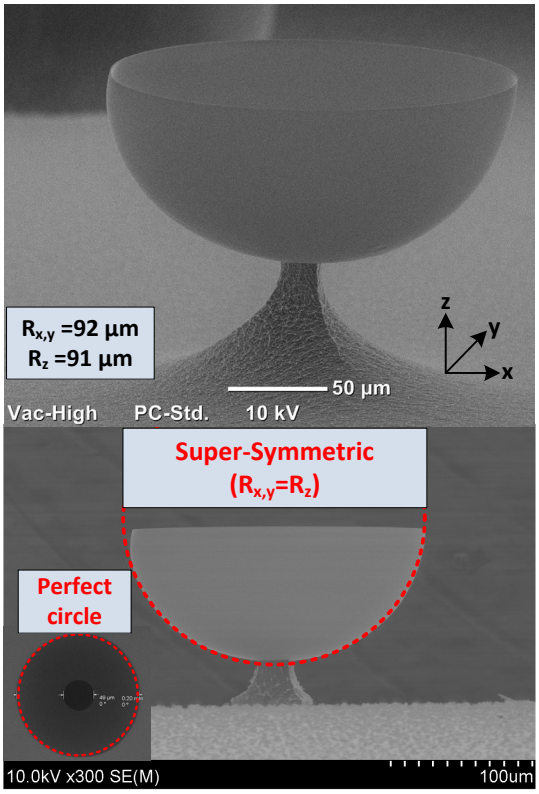

Figure 3: SEM pictures of HSRs fabricated with the pop-up ring mask. The device has a SiO_2 hemispherical shell with a diameter of 180 µm, demonstrating a 3D symmetry of 99%.

EXPERIMENTAL RESULTS

Figure 4 presents experimental setup used to characterize the HSRs. The HSR chip is mounted on a PZT substrate with a carbon tape and excited using a signal generator inside a Karl Suss vacuum probe station. The resonator edge motion is detected by using a LDV and Zurich lock-in amplifier. Figure 5 (a-b) shows fundamental modes without any spurs and frequency split between two degenerate n=2 modes as 512 Hz, showing asymmetry of 0.5%. Ring down tests have been performed to accurately measure the Q of the HSRs. Figure 5 (c) presents ring down measurement of a HSR at 25 µTorr, showing decay rate (τ) of 100 ms which correponds to a Q of 31542 for n=2 mode.

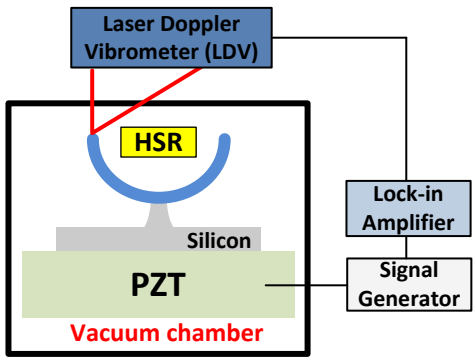

Figure 4: HSR is characterized inside a Karl Suss vacuum probe station at 25 µTorr. Resonator edge motion is measured with a LDV and Zurich lock-in.

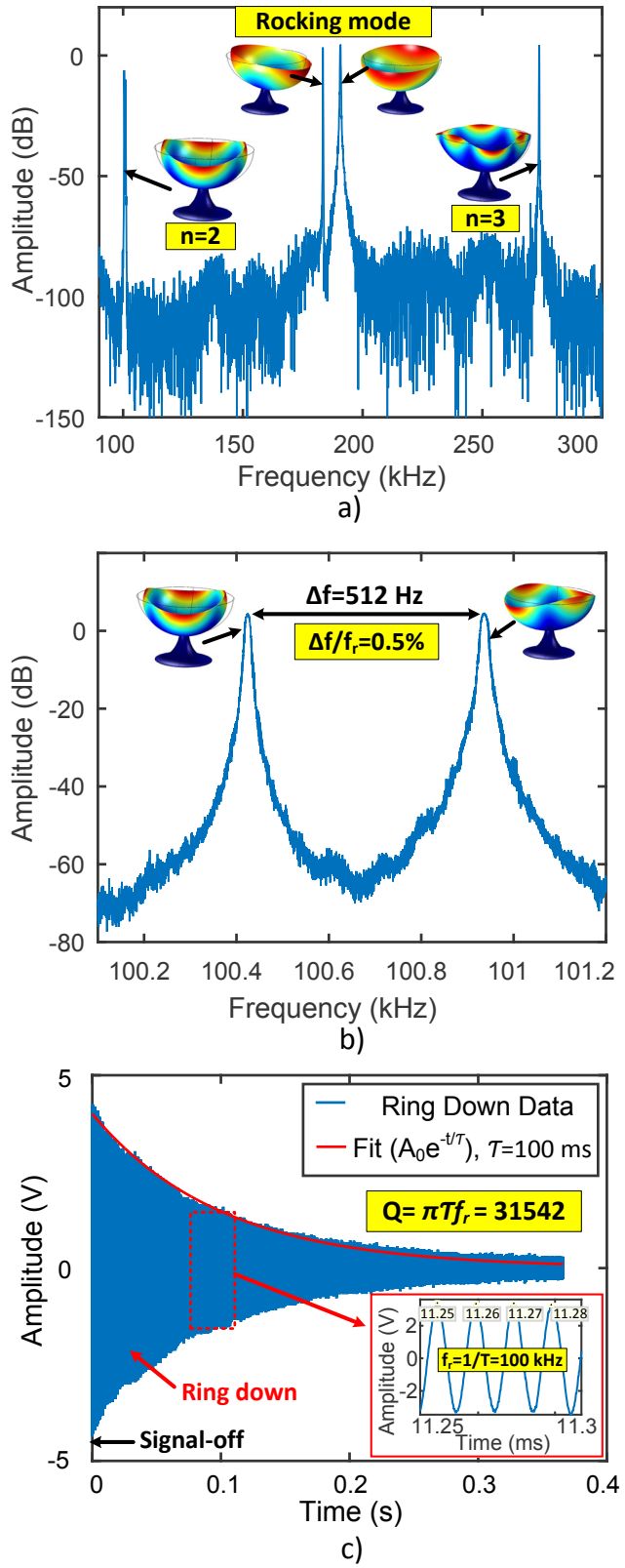

Figure 5: Measurement results of a HSR fabricated using the pop-up ring mask: (a) Frequency response showing first three (n=2, rocking, and n=3) modes with no spurs. (b) Zoom-in view of the n=2 modes, showing a frequency split (Δf) of 512 Hz between two degenerate modes. (c) Ring down measurement of the HSR at 25 μTorr, showing decay rate (τ) of 100 ms which correponds to a Q of 31542 for n=2 mode.

Table 1 summarizes the measurement results for an HSR chip fabricated using the pop-up ring mask. Frequency split (Δf) between two degenerate n=2 modes increases for the devices at the edge of the chip whereas it is minimum for the devices at the center of the chip. Figure 6 presents an SEM image of the HSR array showing a spread in the anchor dimensions due to the XeF_2 release conditions. The anchor dimensions become smaller for the devices at the edge of the chip since they are etched faster compared to the ones at the center during XeF_2 process. As the anchor becomes smaller, it also becomes asymmetic resulting a higher frequency split. This result shows that additional design and fabrication innovations are necessary to achieve chip-scale and wafer-scale fabrication tolerance of $R_z/R_{x,y}$ better than 99%.

Table 1: Summary of the measurement results for an HSR chip fabricated using the pop-up ring mask. Frequency split (Δf) becomes minimum for the HSR at the center of the chip (Device #4).

Device #	***1***	***2***	***3***	***4***	***5***	***6***
$f_{1,\,n=2}$ ***(kHz)***	92.6	97.8	98.4	100.4	98.5	97.7
$f_{2,\,n=2}$ ***(kHz)***	95.2	99.0	99.4	100.9	99.4	99.9
Δf ***(kHz)***	2.6	1.2	1	0.5	0.9	2.2
$\Delta f/f_r$ ***(%)***	2.8	1.22	0.98	0.5	0.9	2.2
$f_{rocking}$ ***(kHz)***	106	165	199	183	158	131

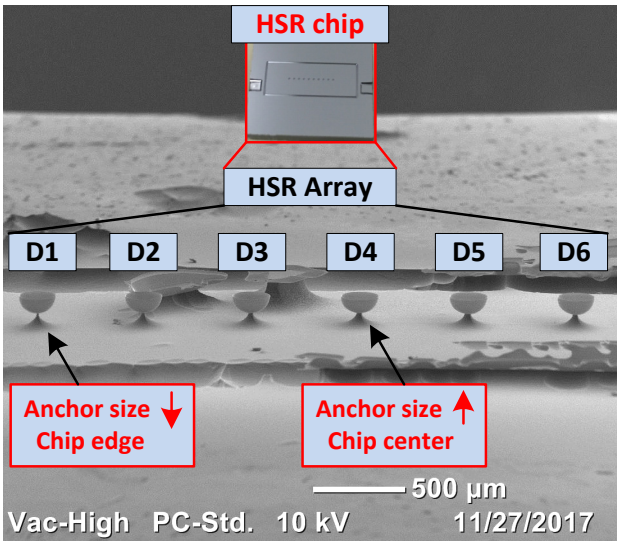

Figure 6: SEM image of the HSR array showing a spread in the anchor dimensions where anchors become smaller at the edge of the chip due to the XeF_2 release conditions. The chip got contaminated during testing of the HSRs.

FEM simulations are performed in COMSOL to analyze acceleration sensitivity of different HSR structures where a static acceleration of 50000 m/s^2 is applied along x or z axis. The applied acceleration causes a mechanical deformation in the structure and results a shift in the resonance frequency. Figure 7 shows resonance frequency shift due to lateral or vertical acceleration induced

mechanical stress for different HSR structures. Lateral acceleration sensitivity increases from shallower to deeper structures whereas the exact opposite is valid for the vertical acceleration. Table 2 presents the summary of acceleration insensitivity simulations performed in COMSOL.

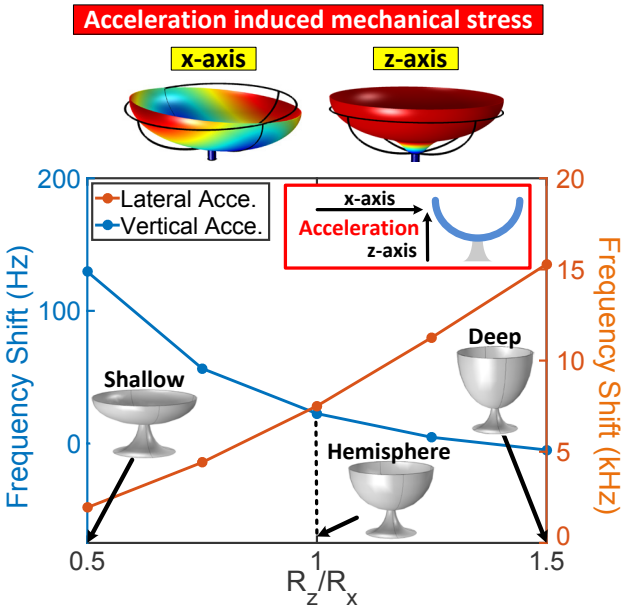

Figure 7: Frequency shift for different HSR structures due to acceleration induced mechanical stress simulated in COMSOL. Hemisphere combines the advantages of both shallower and deeper structures, showing an excellent insensitivity for simultaneous x-z axis acceleration.

Table 2: Summary of acceleration insensitivity simulations performed in COMSOL.

Structure	***Acceleration Insensitivity***		
	In-plane (a_x ***or*** a_y)	***Out-of-plane*** (a_z)	$\overrightarrow{a_x} \times \overrightarrow{a_z}$
Shallow	Best	Bad	Bad
Hemisphere	Good	Good	Excellent
Deep	Bad	Best	Bad

CONCLUSIONS

In this work, we present a new method for the fabrication of highly symmetric and smooth silicon molds based on HNA etching of <111> silicon using a pop-up ring mask without increasing the process steps or complexity. Proper design of these pop-up rings allows excellent control of lateral and vertical etch rates, enabling the fabrication of high Q (31542) and super-symmetric (3D symmetry of 99%) HSRs. Although the process yield is very high, non-uniformity in the XeF_2 release should be minimized for batch-fabricated HSR devices. FEM simulations have been performed to analyze the acceleration sensitivity of the different HSR structures. Super-symmetric HSRs fabricated using the pop-up ring mask shows an excellent acceleration insensitivity in both x and z axis. The authors will focus on minimizing non-uniformity in the XeF_2 release, fabrication of mm-scale HSRs and acceleration sensitivity measurements as a future work.

ACKNOWLEDGEMENTS

The authors would like to thank Professor Jeffrey Rhoads and Dr. Nikhil Bajaj for their invaluable discussions on experimental testing of HSRs. The authors also gratefully acknowledge Michael D. Sinanis and Dr. Nithin Raghunathan for many helpful discussions on the fabrication process.

REFERENCES

[1] A. A. Trusov, M. R. Phillips, A. Bettadapura, G. Atikyan, G. H. McCammon, J. M. Pavell, Y. A. Choi, D. K. Sakaida, D. Rozelle, and A. D. Meyer, "mHRG: Miniature CVG with Beyond Navigation Grade Performance and Real Time Self-Calibration", *IEEE Inertial Sensors 2016,* pp.29-32.

[2] J. J. Bernstein, M. G. Bancu, E. H. Cook, M. V. Chaparala, W. A. Teynor, and M. C. Weinberg, "A MEMS Diamond Hemispherical Resonator", *J. Micromech. Microeng,* Vol. 23, 125007, 2013.

[3] A. Bhat, L. C. Fegely, and S. Bhave, "GOBLIT: A Giant Opto-Mechanical Bulk Machined Light Transducer", *Hilton Head 2014*, pp.247-250.

[4] L. D. Sorenson, X. Gao, and F. Ayazi, "3-D Micromachined Hemispherical Shell Resonators with Integrated Capacitive Transducers", *IEEE MEMS 2012*, pp. 168-171.

[5] A. Heidari, M. L. Chan, H. A. Yang, G. Jaramillo, P. T. Tehrani, P. Fonda, H. Najar, K. Yamazaki, L. Lin, and D. A. Horsley, "Micromachined Polycrstalline Diamond Hemispherical Shell Resonators", *Transducers 2013*, pp. 2415-2418.

[6] S. A. Zotov, A. A. Trusov, and A. M. Shkel, "Three-Dimensional Spherical Shell Resonator Gyroscope Fabricated Using Wafer-Scale Glassblowing", *J. Microelectromech. Syst.*, vol. 20, pp. 691-701, 2011.

[7] J. Y. Cho, J. Woo, J. Yan, R. L. Peterson, and K. Najafi, "Fused-Silica Micro Birdbath Resonator Gyroscope", *J. Microelectromech. Syst.*, vol. 23, pp. 66-77, 2014.

[8] D. Saito, C. Yang, A. Heidari, H. Najar, L. Lin, and D. A. Horsley, "Batch-Fabricated High Q-Factor Microcrystalline Diamond Cylindrical Resonator", *IEEE MEMS 2015*, pp. 801-804.

[9] C. Zhang, A. Cocking, E. Freeman, Z. Liu, and S. Tadigadapa, "Whispering Gallery Mode Based On-Chip Glass Microbubble Resonator for Thermal Sensing", *Transducers 2017*, pp. 630-633.

[10] B. Hamelin, V. Tavassoli, and F. Ayazi, "Microscale Pierced Shallow Shell Resonators: A Test Vehicle to Study Surface Loss", *IEEE MEMS 2017*, pp. 1134-1137.

[11] L. C. Fegely, D. N. Hutchinson, and S. A. Bhave, "Isotropic Etching of 111 SCS for Wafer-Scale Manufacturing of Perfectly Hemispherical Silicon Mold", *Transducers 2011*, pp. 2295-2298.

CONTACT

*Mustafa Mert Torunbalci, mobile: +1-765-418-8559; mtorunba@purdue.edu